RAPID COMMUNICATION

Two-coupled structural modulations in charge-density-wave state of $SrPt_2As_2$ superconductor*

Wang Li(王 莉)[a], Wang Zhen(王 臻)[a], Shi Hong-Long(施洪龙)[a,b], Chen Zhen(陈 震)[a], Chiang Fu-Kuo(蒋复国)[a], Tian Huan-Fang(田焕芳)[a], Yang Huai-Xin(杨槐馨)[a], Fang Ai-Fang(房爱芳)[a], Wang Nan-Lin(王楠林)[a], and Li Jian-Qi(李建奇)[a]†

[a] *Beijing National Laboratory for Condensed Matter Physics, Institute of Physics, Chinese Academy of Sciences, Beijing* 100190, *China*
[b] *School of Science, Minzu University of China, Beijing* 100081, *China*

(Received 11 March 2014; revised manuscript received 16 May 2014; published online 10 June 2014)

Transmission electron microscopy (TEM) study of $SrPt_2As_2$ reveals two incommensurate modulations appearing in the charge-density-wave (CDW) state below $T_{CDW} \approx 470$ K. These two structural modulations can be well explained in terms of condensations of two-coupled phonon modes with wave vectors of $\boldsymbol{q}_1 = 0.62\boldsymbol{a}^*$ on the $\boldsymbol{a}^*$–$\boldsymbol{b}^*$ plane and $\boldsymbol{q}_2 = 0.23\boldsymbol{a}^*$ on the $\boldsymbol{a}^*$–$\boldsymbol{c}^*$ plane. The atomic displacements occur along the $\boldsymbol{b}$-axis direction for $\boldsymbol{q}_1$ and along the $\boldsymbol{c}$-axis direction for $\boldsymbol{q}_2$, respectively. Moreover, the correlation between $\boldsymbol{q}_1$ and $\boldsymbol{q}_2$ can be generally written as $\boldsymbol{q}_1 = (\boldsymbol{q}_2 + \boldsymbol{a}^*)/2$ in the CDW state, suggesting the presence of essential coupling between $\boldsymbol{q}_1$ and $\boldsymbol{q}_2$. A small fraction of Ir doping on the Pt site in $Sr(Pt_{1-x}Ir_x)_2As_2$ ($x \leq 0.06$) could moderately change these CDW modulations and also affect their superconductivities.

Keywords: superconductivity, charge-density-wave, structural modulation, transmission electron microscopy

PACS: 61.05.J–, 74.70.Xa, 71.45.Lr, 61.50.Ah **DOI:** 10.1088/1674-1056/23/8/086103

1. Introduction

The superconductivity and structural properties of AFe_2As_2 (A = alkaline-earth metals, $ThCr_2Si_2$-type) have been extensively investigated since the discovery of high-T_c superconductivity at $T_c = 26$ K in LaFeAsO(F).[1] The parent phase AFe_2As_2 could exhibit superconductivity either by chemical doping or under a high pressure to suppress the antiferromagnetic property.[2–8] Recent investigations show that the 5d-transion metal Pt pnictide $SrPt_2As_2$ with the $CaBe_2Ge_2$-type structure shows a superconducting transition at a temperature of 5.2 K,[9,10] moreover, the $SrPt_2As_2$ compound shows a notable charge-density-wave (CDW) transition accompanied with a structural transformation at around 470 K.[9,10] In contrast with the well-known $ThCr_2Si_2$-type structure, $CaBe_2Ge_2$-type crystals have non-centrosymmetric structures. Taking $SrPt_2As_2$ for example, it has a visible layered structure with the –As–Pt–As– layers and the –Pt–As–Pt– layers stacking alternately along the $\boldsymbol{c}$-axis direction. Actually, the CDW instability in low-dimensional metal has been investigated as the significant issue for decades; however, the CDW transitions as observed in the two-dimensional systems are still intensely debated issues. According to first-principles calculations, the $CaBe_2Ge_2$-type $SrPt_2As_2$ is a unique system with an "intermediate"-type Fermi surface containing remarkable hole pockets,[11] this feature could play a critical role in understanding the properties of CDW and superconductivity as observed in the present system. In addition, it was also proposed that the CDW can enhance the superconductivity in an electron–phonon coupled system,[12,13] and therefore, the superconductivity and CDW can coexist in one system.[14–16] In recent investigations, experimental measurements of the structural and physical properties have been performed on the well-characterized $Sr(Pt_{1-x}Ir_x)_2As_2$ ($x = 0,\ 0.06$) single crystals.[10] It is demonstrated that a structural transition from tetragonal to orthorhombic phase occurs at about 470 K in $SrPt_2As_2$ and becomes lower in the $Sr(Pt_{0.94}Ir_{0.06})_2As_2$ material.[10] Below this critical temperature, a structural modulation in association with the CDW appears along the $\boldsymbol{a}$-axis direction, careful structural study shows that the CDW occurs in the –As–Pt–As– layers and often exhibits an incommensurate periodicity.[9,10,17]

In the present paper, we report on our study of the microstructure of $Sr(Pt_{1-x}Ir_x)_2As_2$ ($x = 0, 0.06$) by transmission electron microscopy. We find that the structural distortions in the CDW state can be well characterized by two incommensurate transverse waves: i.e., the $\boldsymbol{q}_1 = 0.62\boldsymbol{a}^*$ which shows a similar periodicity to that observed in X-ray diffraction,[17] and a new modulation that can be written as $\boldsymbol{q}_2 = 0.23\boldsymbol{a}^*$. *In situ* TEM observations show that both structural modulations become invisible at temperatures above T_{CDW}.

*Project supported by the National Basic Research Program of China (Grant Nos. 2011CBA00101, 2010CB923002, 2012CB821404, and 2011CB921703), the National Natural Science Foundation of China (Grant Nos. 11190022, 11274368, and 51272277), and the Funds from the Chinese Academy of Sciences.

†Corresponding author. E-mail: ljq@aphy.iphy.ac.cn

© 2014 Chinese Physical Society and IOP Publishing Ltd

2. Experiment

Single crystals of $SrPt_2As_2$ and $Sr(Pt_{0.94}Ir_{0.06})_2As_2$ samples used in the present study were synthesized by a self-melting technique.[10] The crystal structure and fundamental physical properties for all samples were first characterized by X-ray diffraction and measurements of physical properties.[10] Microstructure investigations were performed on an FEI Tecnai-F20 transmission electron microscope equipped with double-tilt heating and cooling holders. The TEM samples were prepared by crushing the single crystals, and then the resulting suspensions were dispersed on a holey copper grid coated with a thin carbon film. Image simulation structural analyses were performed by using the MACTEMPAS software.

3. Results and discussion

In order to understand the microstructure features in the CDW state of the $SrPt_2As_2$ material, particularly the fundamental properties of CDW modulation, we have performed an extensive experimental investigation by selected-area electron diffraction (SAED) and high-resolution transmission electron microscopy. Figures 1(a)–1(d) show electron-diffraction patterns taken along the relevant [001], [010], [011], and [100] zone-axis directions at room temperature, respectively. In order to compare the measured patterns with the simulated patterns described in the following text, we use the electron beam incident direction for indexing the diffraction patterns. The main diffraction spots with relatively strong intensity in all patterns can be well indexed by the known orthorhombic structure with the space group of *Pmmn* (No. 59) and lattice parameters of $a = 4.470$ Å, $b = 4.497$ Å, and $c = 9.816$ Å, which are in good agreement with the X-ray diffraction results.[17] On the other hand, our structural analysis shows that the two sets of satellite spots corresponding to two distinctive structural modulations commonly appear in our experimental observations, as is clearly illustrated in Figs. 1(a) and 1(b), respectively. It is noted that the $\boldsymbol{q}_1$ modulation with a wave vector of $\boldsymbol{q}_1 = 0.62\boldsymbol{a}^*$ shows up certain similar features as observed by using X-ray diffraction in the previous literature.[17] In addition, there is a new structural modulation ($\boldsymbol{q}_2$) existing in many diffraction patterns, and the $\boldsymbol{q}_2$ modulation in general has a relatively weak intensity and can be clearly observed along the [010] zone-axis direction. This modulation wave can be written as $\boldsymbol{q}_2 = 0.23\boldsymbol{a}^*$. Actually, coexistence of these two modulations ($\boldsymbol{q}_1$ and $\boldsymbol{q}_2$) can be seen along several main zone-axis directions as shown in the diffraction pattern of Fig. 1(c), it was taken along the [011] zone-axis direction. Though the $\boldsymbol{q}_2$ modulation also goes along the $\boldsymbol{a}$-axis direction, it actually exhibits notable different polarization from the $\boldsymbol{q}_1$ modulation. In order to facilitate the comparisons between the $\boldsymbol{q}_1$ and $\boldsymbol{q}_2$ modulations, a series of selected-area electron diffraction patterns and TEM images has been obtained in a few well characterized crystals. Our observations show that the structural distortion in the CDW state of $SrPt_2As_2$ can be characterized by two incommensurate transverse waves of $\boldsymbol{q}_1 = 0.62\boldsymbol{a}^*$ on the $\boldsymbol{a}^*$–$\boldsymbol{b}^*$ plane and $\boldsymbol{q}_2 = 0.23\boldsymbol{a}^*$ on the $\boldsymbol{a}^*$–$\boldsymbol{c}^*$ plane, and that the atomic displacements in both modulations occur in the direction perpendicular (or right angled) to the $\boldsymbol{a}$-axis direction (i.e., the wave vector direction). For instance, the $\boldsymbol{q}_2$ modulation can be regarded as a transverse wave with the incommensurate period of around $4.2\boldsymbol{d}_{100}$ and, therefore, can be clearly viewed along the [010] zone-axis direction. Moreover, our *in situ* TEM observations from 20 K up to 500 K suggest that the relationship between $\boldsymbol{q}_1$ and $\boldsymbol{q}_2$ can be generally written as $\boldsymbol{q}_1 = (\boldsymbol{q}_2 + \boldsymbol{a}^*)/2$ as discussed in the following context. This fact likely suggests the presence of essential coupling between these two modulations.

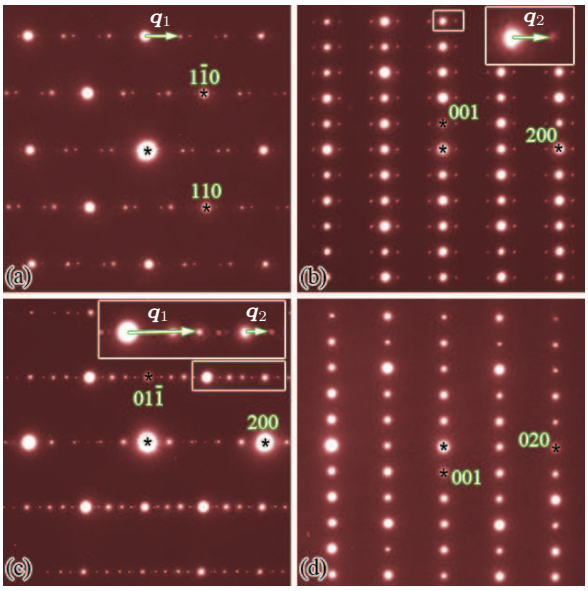


Fig. 1. (color online) Electron diffraction patterns of $SrPt_2As_2$ along relevant directions. (a) Electron diffraction pattern taken along the electron beam incident direction [001] showing the $\boldsymbol{q}_1$ modulation on the $\boldsymbol{a}^*$–$\boldsymbol{b}^*$ reciprocal plane; (b) the $\boldsymbol{q}_2$=0.23$\boldsymbol{a}^*$ modulation on the $\boldsymbol{a}^*$–$\boldsymbol{c}^*$ plane; (c) the coexistence of $\boldsymbol{q}_1$ and $\boldsymbol{q}_2$ modulations observed along the electron beam incident direction [011]. (d) Electron diffraction pattern taken along the electron beam incident direction [100], no modulation spots are observable.

Now we proceed to discuss the condensations of phonon modes and examine the local atomic structural distortions following with the CDW. We first perform our theoretical simulation for CDW modulations based on the experimental data reported by Imre *et al.*[17] The superstructure cell used in the present calculations for the CDW modulation adopts the wave vector of $\boldsymbol{q}_1 \approx 0.6\boldsymbol{a}^*$ and lattice parameters of $a = 22.350$ Å, $b = 4.497$ Å, and $c = 9.816$ Å. Figures 2(a) and 2(b) show the theoretical diffraction patterns along the [001] and [010] zone-axis directions, respectively. It is recognizable that in comparison with experimental results of Fig. 1, the simulated diffraction pattern in Fig. 2(a) is likely to match qualitatively with the experimental one (Fig. 1(a)). However, the theoretical diffraction pattern of Fig. 2(b) shows notable satellite spots

in stark contrast with the experimental diffraction pattern of Fig. 1(b) in which a series of satellite spots from the new $\boldsymbol{q}_2$ modulation is observable.

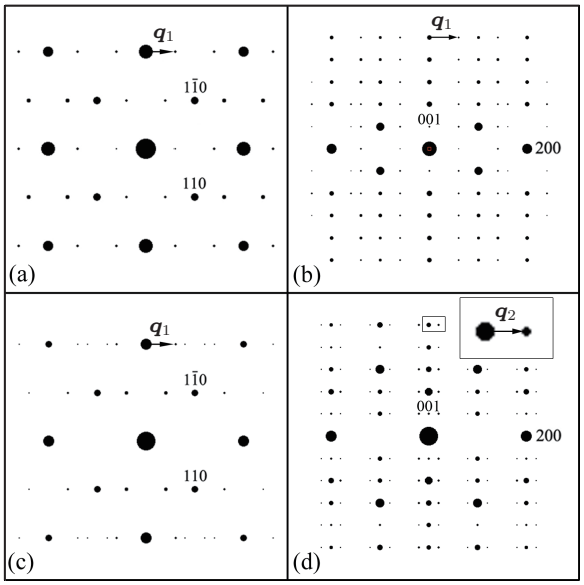


Fig. 2. Theoretical electron diffraction patterns of $\boldsymbol{a}^*$–$\boldsymbol{b}^*$ and $\boldsymbol{a}^*$–$\boldsymbol{c}^*$ planes for CDW modulation. (a) and (b) Simulated patterns for a structural model based on X-ray diffraction. (c) and (d) Simulated patterns based on model with $\boldsymbol{q}_1$ and $\boldsymbol{q}_2$ transverse waves. These patterns are fundamentally in agreement with the experimental ones.

According to a careful structural analysis of $SrPt_2As_2$, we find that structural distortions in CDW state of $SrPt_2As_2$ can be fundamentally explained by two remarkable incommensurate modulations along the $\boldsymbol{a}$-axis direction: the $\boldsymbol{q}_1$ modulation that corresponds to a transverse wave with atomic displacement along the $\boldsymbol{b}$-axis direction, and $\boldsymbol{q}_2$ modulation that is also a transverse wave with the atomic displacement along the $\boldsymbol{c}$-axis direction. In addition, the correlation between these two modulations is governed by $\boldsymbol{q}_1 = (\boldsymbol{q}_2 + \boldsymbol{a}^*)/2$. In order to facilitate theoretical calculations of superstructure modulation, we perform our careful analysis on two models with $\boldsymbol{q}_1 \approx 0.6\boldsymbol{a}^*$ and $\boldsymbol{q}_2 \approx 0.2\boldsymbol{a}^*$, (the supercell $5a \times b \times c$ is created with parameters $a_s = 5a = 22.35$ Å, $b_s = b = 4.497$ Å, and $c_s = c = 9.816$ Å). The $\boldsymbol{q}_1$ and $\boldsymbol{q}_2$ modulations are mainly induced by the atomic displacements in the layers of the $PtAs_4$ tetrahedron, and the other atoms with less displacement affected by the modulations are neglected in the present calculation. Following the sinusoidal modulations, the atomic position and displacement in the –As–Pt–As– layer are given as follows. For $\boldsymbol{q}_1$ modulation, the position of the atom after shifting along the $\boldsymbol{b}$-axis is given by

$$y_s^i = y^i + U_y \sin(5 \times 2\pi \boldsymbol{q}_1 \cdot \boldsymbol{r}^i + \varphi_y), \quad (1)$$

for $\boldsymbol{q}_2$ modulation, the position of the atom after displacing along the $\boldsymbol{c}$-axis is given by

$$z_s^i = z^i + U_z \sin(5 \times 2\pi \boldsymbol{q}_2 \cdot \boldsymbol{r}^i + \varphi_z), \quad (2)$$

where x^i, y^i, and z^i denote the undistorted position of the i-th atom in the $PtAs_4$ tetrahedron of the superstructure, U_y and U_z indicate the amplitudes of the sinusoidal modulation wave along the $\boldsymbol{b}$ and $\boldsymbol{c}$ axes, and φ_y and φ_z refer to initial phases of the sinusoidal modulation waves for $\boldsymbol{q}_1$ and $\boldsymbol{q}_2$. Since $\boldsymbol{q}_1 \approx 0.6\boldsymbol{a}^*$ and $\boldsymbol{q}_2 \approx 0.2\boldsymbol{a}^*$, atomic displacements along the $\boldsymbol{b}$ axis and $\boldsymbol{c}$ axis could be recognized in terms of $U_y \sin(6\pi x^i + \varphi_y)$ and $U_z \sin(2\pi x^i + \varphi_z)$, respectively. According to our experimental data, the Pt displacements in two modulations are estimated in percentage terms to be $U_y \approx 3\%$, and $U_z \approx 1\%$, and φ_y and φ_z are assumed to be 0; for displacements of As atoms, U_y is estimated to be about 2% with $\varphi_y = \pi$, and U_z is estimated to be 1% with $\varphi_z = 0$. As a result, the simulated patterns in Figs. 2(c) and 2(d) can be well consistent with our experimental data. We have analyzed the reflection conditions associated with the $\boldsymbol{q}_1$ and $\boldsymbol{q}_2$ modulations by using the super-space group analysis,[18,19] and we can conclude that the $\boldsymbol{q}_1$ and $\boldsymbol{q}_2$ modulations are essentially independent, but with certain cooperative structural properties.

A better and clear view of atomic displacements for the $\boldsymbol{q}_1$ and $\boldsymbol{q}_2$ modulations can be obtained by high-resolution TEM observations along the $\boldsymbol{c}$-axis and $\boldsymbol{b}$-axis directions, respectively. Figure 3(a) shows the high-resolution TEM image taken along the [001] zone-axis direction for $SrPt_2As_2$ single crystal sample, in which the $\boldsymbol{q}_1$ modulation wave is clearly seen. Figure 3(b) shows a simplified structural model illustrating the displacements of Pt atoms associated with a sinusoidal modulation; a theoretical simulation image is also shown in Fig. 3(c) for comparison, in which periodic contrast changes arising from structural modulation are in good agreement with the experimental ones. Figure 3(d) shows a high-resolution TEM image taken along the [010] zone-axis direction, in which the structural modulation corresponding to the modulated vector $\boldsymbol{q}_2 = 0.23\boldsymbol{a}^*$ can be clearly read out. The curve of intensity in Fig. 3(d) shows that the wavelength of modulation wave is about 2.09 nm. Figures 3(e) and 3(f) show the schematic structural model and a theoretical image for the $\boldsymbol{q}_2$ modulation. It is noted that atomic displacements in association with structural modulations can be observed in all experimental and theoretical images.

Measurements of transport properties of the $SrPt_2As_2$ crystal often reveal a visible resistivity anomaly in association with the CDW transition at about 470 K.[10] In our *in situ* TEM experimental observations, the temperature dependences of both $\boldsymbol{q}_1$ and $\boldsymbol{q}_2$ modulations have been carefully examined. Figures 4(a)–4(f) show a series of diffraction patterns taken along the [001] and [010] zone-axis directions in a temperature range from 300 K up to 500 K, illustrating the changes of superstructure spots. It is recognizable that the intensities of the superstructure spots decrease progressively with the increase of temperature, and the superstructure spots characterized by $\boldsymbol{q}_1$ and $\boldsymbol{q}_2$ completely disappear above 470 K and 450 K, respectively. We notice that $\boldsymbol{q}_1$ and $\boldsymbol{q}_2$ modulations disappear

at slightly different temperatures, this fact likely suggests that the complex structural dynamic instability appears following the CDW transitions, and, as a result, the $\boldsymbol{q}_2$ modulation turns stable after the $\boldsymbol{q}_1$ modulation has become stable. Our *in situ* TEM investigation also reveals that this CDW transition is fundamentally reversible, and no significant changes in their periodicities are observed in the whole high temperature range. On the other hand, we also perform the *in situ* cooling TEM experimental observations from room temperature down to 20 K, and no remarkable structural alteration is observed.

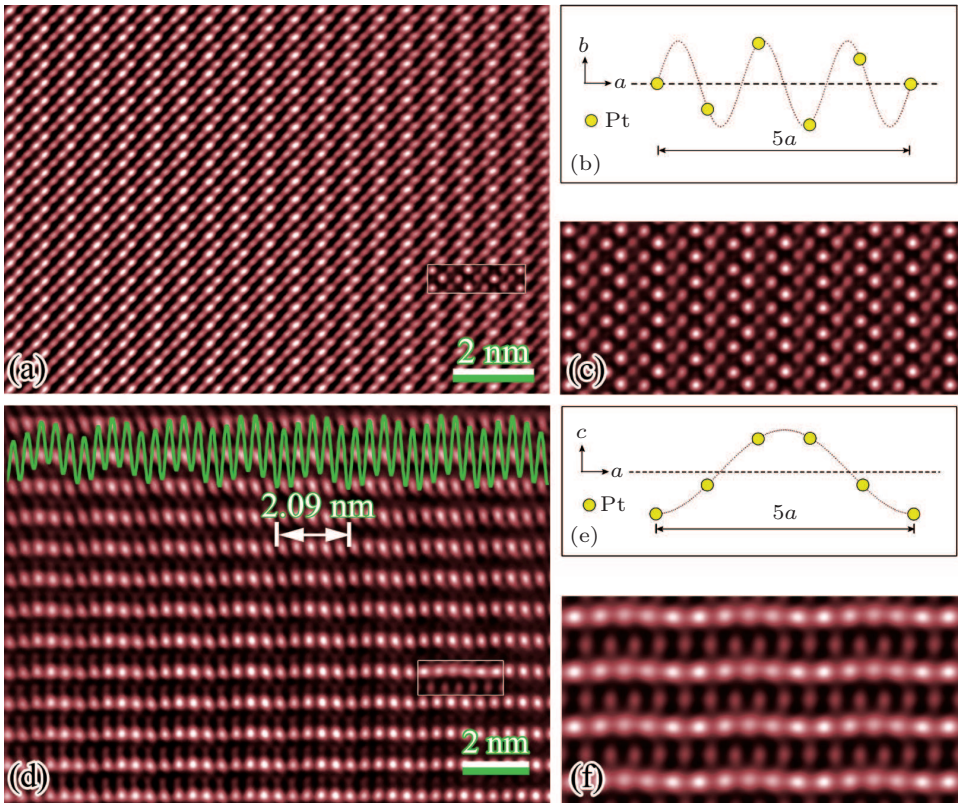


Fig. 3. (color online) High-resolution TEM images of $SrPt_2As_2$ taken along (a) the electron beam incident direction [001] and (d) the electron beam incident direction [010]. Schematic illustrations of the Pt atomic displacements in –As–Pt–As– layers (b) along the $\boldsymbol{b}$ axis for $\boldsymbol{q}_1$ modulation and (e) along the $\boldsymbol{c}$ axis for $\boldsymbol{q}_2$ modulation. Theoretical simulated images for these two modulations are shown in panels (c) and (f), respectively.

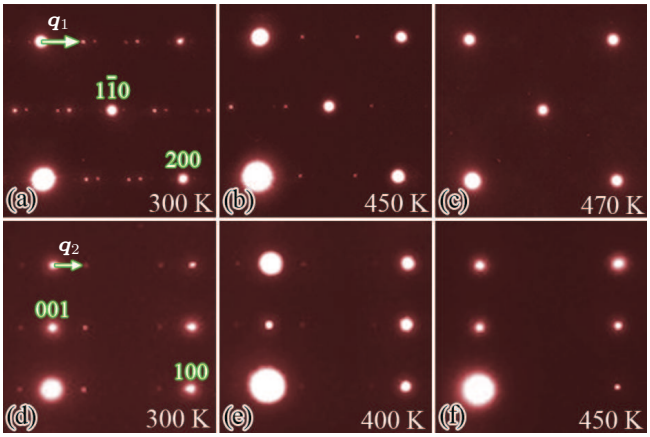


Fig. 4. (color online) The temperature dependences of the superstructure reflections from 300 K to 500 K, (a)–(c) electron diffraction patterns taken along the electron beam incident direction [001], and (d)–(f) electron diffraction patterns taken along the electron beam incident direction [010]. The intensities of superstructure spots become weaker with the increase of temperature and disappear above 470 K (Fig. 4(c)) and 450 K (Fig. 4(f)), respectively.

It is expected that a small fraction substitution of Pt by certain relative elements in this layered material could tune an electronic structure near the Fermi level, the CDW transition and superconductivity as well. The experimental measurements show that the Ir-doped $Sr(Pt_{0.94}Ir_{0.06})_2As_2$ can yield visible changes of the critical temperatures of the CDW and superconducting transitions as schematically shown in Fig. 5(a), in which the resistivity anomaly in a $Sr(Pt_{0.94}Ir_{0.06})_2As_2$ crystal occurs at near 375 K, and the superconducting transition temperature decreases to 4.73 K.[10] TEM observations show that the Ir doping could also result in a tendency to increase the period of superstructure modulation and reduce the intensity for both $\boldsymbol{q}_1$ and $\boldsymbol{q}_2$ modulations in comparison with what are observed in $SrPt_2As_2$. Figures 5(b) and 5(c) show two typical electron diffraction patterns taken along the [001] and [010] zone-axis directions at room temperature respectively. It is demonstrated that the intensity of the superstructure spots decreases and the periods of modulation waves change slightly as characterized by $\boldsymbol{q}_1 = 0.60\boldsymbol{a}^*$

and $\boldsymbol{q}_2 = 0.19\boldsymbol{a}^*$, respectively. Moreover, it is also noted that the correlation between $\boldsymbol{q}_1$ and $\boldsymbol{q}_2$ can also be written as $\boldsymbol{q}_1 = (\boldsymbol{q}_2 + \boldsymbol{a}^*)/2$. Though the essential effect of CDW on the low-temperature superconductivity is still a debated issue as discussed in some literature, it is commonly believed that the variation of electronic structure, such as the electron distribution near the Fermi surface, could result in visible changes in the CDW state and superconductivity.[12–16]

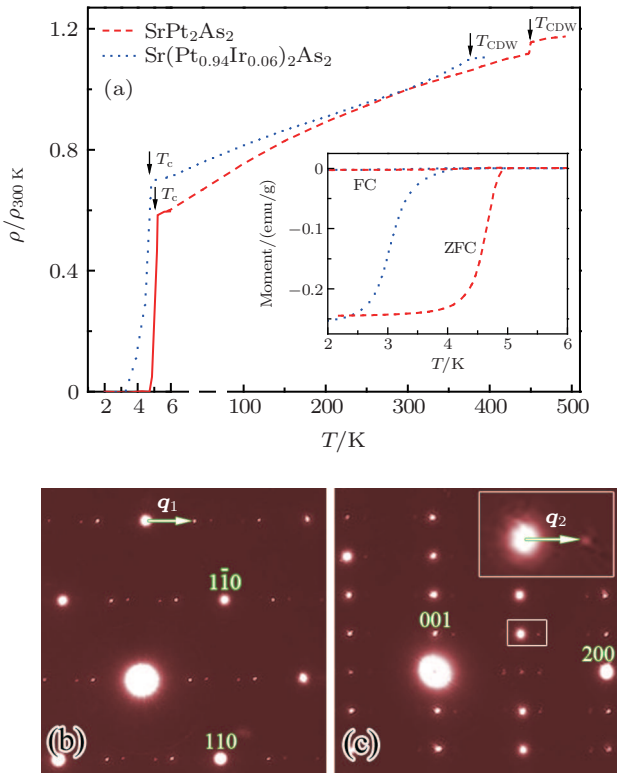


Fig. 5. (color online) Effects of Ir doping on the CDW modulation and superconductivity. (a) Schematic illustrations of resistivity (normalized by the value at 300 K) and magnetizations for $SrPt_2As_2$ and $Sr(Pt_{0.94}Ir_{0.06})_2As_2$, exhibiting clear anomalies at CDW transitions and superconducting transitions (Ref. [10]). (b) and (c) Electron diffraction patterns of $Sr(Pt_{0.94}Ir_{0.06})_2As_2$, showing that the $\boldsymbol{q}_1$ and $\boldsymbol{q}_2$ modulations become weaker than those in Figs. 1(a) and 1(b) for $SrPt_2As_2$.

The essential structural features of $SrPt_2As_2$ in correlation with the coexistence of CDW and superconductivity have aroused a lot of interest in past years, it was suggested that the CDW could enhance superconductivity in certain electron–phonon coupled systems.[12,13] Actually, Fermi surface nesting is revealed as a strong candidate for driving CDW formations in a variety of low-dimensional systems, and the magnitudes of nesting vector obtained in certain systems are in excellent agreement with theoretical data.[20] However, the behavior in an incommensurate case is much less clear, and complex structural variation and microstructural phenomena often appear following the CDW transitions, such as antiphase boundaries and discommensurations.[21,22] From the structural point of view, the typical structural modulations in the CDW state can be well explained in terms of the condensation of the phonon modes,[23] the amplitudes of the relevant phonon modes are temperature-dependent as observed for $SrPt_2As_2$. It is well established that the frequencies of these phonon modes decrease as the temperature lowers to T_{CDW}, and the restoring forces at T_{CDW} for these modes vanish so that the atoms shift to new equilibrium positions, then this transition could result in the visible structural modulations in the CDW state as indicated in our TEM observations. It is remarkable that our observations evidently suggest the presence of condensation of two coupled phonon modes in this layered system, and it is expected that this feature is also important for understanding the physical properties in this kind of material, for instance, the electron–charge coupling as a central issue has extensively been discussed in studies of change/orbital ordering in manganese and charge–stripe structures in high-T_c superconductors.[24,25] It is also noted that these properties could also be significant for understanding the superconductivity appearing in $SrPt_2As_2$ at a lower temperature, e.g. the two distinctive superconducting gaps have been revealed in the temperature evolution of the electronic specific heat.[26]

4. Conclusions

In summary, layered superconducting $SrPt_2As_2$ material shows a remarkable microstructural feature in its CDW state as revealed by TEM observations. *In situ* TEM observations evidently reveal that there are two transverse modulations commonly existing below the CDW transition. These incommensurate modulations can be written as $\boldsymbol{q}_1 = 0.62\boldsymbol{a}^*$ on the $\boldsymbol{a}^*$–$\boldsymbol{b}^*$ reciprocal plane and $\boldsymbol{q}_2 = 0.23\boldsymbol{a}^*$ on the $\boldsymbol{a}^*$–$\boldsymbol{c}^*$ plane, it also noted that the correlation between $\boldsymbol{q}_1$ and $\boldsymbol{q}_2$ can be also written as $\boldsymbol{q}_1 = (\boldsymbol{q}_2 + \boldsymbol{a}^*)/2$. The presence of two coupled modulations in CDW states suggests novel properties for phonon condensation in this layered system. The CDW modulations and superconductivity show slight changes in $Sr(Pt_{1-x}Ir_x)_2As_2$ ($x \leq 0.06$) due to Ir doping for Pt.

References

[1] Kamihara Y, Watanabe T, Hirano M and Hosono H 2008 *J. Am. Chem. Soc.* **130** 3296
[2] Torikachvili M S, Bud'ko S L, Ni N and Canfield P C 2008 *Phys. Rev. Lett.* **101** 057006
[3] Rotter M, Tegel M and Johrendt D 2008 *Phys. Rev. Lett.* **101** 107006
[4] Sefat A S, Jin R, McGuire M A, Sales B C, Singh D J and Mandrus D 2008 *Phys. Rev. Lett.* **101** 117004
[5] Sasmal K, Lü B, Lorenz B, Guloy A M, Chen F, Xue Y Y and Chu C W 2008 *Phys. Rev. Lett.* **101** 107007
[6] Zhu X, Han F, Mu G, Cheng P, Tang J, Ju J, Tanigaki K and Wen H H 2010 *Phys. Rev. B* **81** 104525
[7] Chen G F, Li Z, Li G, Hu W Z, Dong J, Zhou J, Zhang X D, Zheng P, Wang N L and Luo J L 2008 *Chin. Phys. Lett.* **25** 3403
[8] Zhang A M and Zhang Q M 2013 *Chin. Phys. B* **22** 087103
[9] Kudo K, Nishikubo Y and Nohara M 2010 *J. Phys. Soc. Jpn.* **79** 123710

[10] Fang A F, Dong T, Wang H P, Chen Z G, Cheng B, Shi Y G, Zheng P, Xu G, Wang L, Li J Q and Wang N L 2012 *Phys. Rev. B* **85** 184520
[11] Shein I R and Ivanovskii A L 2011 *Phys. Rev. B* **83** 104501
[12] Kiss T, Yokoya T, Chainani A, Shin S, Hanaguri T, Nohara M and Takagi H 2007 *Nat. Phys.* **3** 720
[13] Machida K and Kato M 1987 *Phys. Rev. B* **36** 854
[14] Morosan E, Zandbergen H W, Dennis B S, Bos J W G, Onose Y, Klimczuk T, Ramirez A P, Ong N P and Cava R J 2006 *Nat. Phys.* **2** 544
[15] Zhu X, Lei H and Petrovic C 2011 *Phys. Rev. Lett.* **106** 246404
[16] Sangeetha N S, Thamizhavel A, Tomy C V, Basu S, Awasthi A M, Ramakrishnan S and Pal D 2012 *Phys. Rev. B* **86** 024524
[17] Imre A, Hellmann A, Wenski G, Graf J, Johrendt D and Mewis A 2007 *Z. Anorg. Allg. Chem.* **633** 2037
[18] De Wolff P M, Janssen T and Janner A 1981 *Acta Crystallogr., Sect. A: Cryst. Phys., Diffr., Theor. Gen. Crystallogr.* **37** 625
[19] Henry N F H and Lonsdale K 1969 *International Table for X-ray Crystallography* (Birmingham: Kynoch), Vol. 1
[20] Laverock J, Dugdale S B, Major Zs, Alam M A, Ru N, Fisher I R, Santi G and Bruno E 2005 *Phys. Rev. B* **71** 085114
[21] Chen C H, Gibson J M and Fleming R M 1981 *Phys. Rev. Lett.* **47** 723
[22] Chen C H, Gibson J M and Fleming R M 1982 *Phys. Rev. B* **26** 184
[23] Littlewood P B and Varma C M 1982 *Phys. Rev. B* **26** 4883
[24] Li J Q, Uehara M, Tsuruta C, Matsui Y and Zhao Z X 1999 *Phys. Rev. Lett.* **82** 2386
[25] Tranquada J M, Sternlieb B J, Axe J D, Nakamura Y and Uchida S 1995 *Nature* **375** 561
[26] Xu X, Chen B, Jiao W H, Chen B, Niu C Q, Li Y K, Yang J H, Bangura A F, Ye Q L, Cao C, Dai J H, Cao G and Hussey N E 2013 *Phys. Rev. B* **87** 224507